Macromolecules **2002,** *35,* 827−833

Structure−Property Relations in Dendritic Polyelectrolyte Solutions at Different Ionic Strength

Aissa Ramzi,*,[†] Rolf Scherrenberg,[‡] Jacques Joosten,[‡] Piet Lemstra,[†] and Kell Mortensen[§]

Eindhoven Polymer Laboratories, The Dutch Polymer Institute, Eindhoven University of Technology, P.O. Box 513, NL-5600 MB, Eindhoven, The Netherlands; DSM Research, P.O. Box 18, NL-6160 MD, Geleen, The Netherlands; and Danish Polymer Centre, Risø National Laboratory, DK-4000, Roskilde, Denmark

Received June 20, 2001

ABSTRACT: The structural properties of charged G5 poly(propyleneimine) dendrimers (Astramol) in D_2O solutions have been investigated using small-angle neutron scattering. Upon addition of acid (HCl), the dendrimers become charged, and the scattered patterns exhibit a single correlation peak indicating a spatial arrangement of the molecules in the acidified medium due to the electrostatic repulsion. Its position Q^* is shifted toward wider angles by increasing the dendrimers concentration, leading to a scaling relation $Q^* \sim \phi^{0.32\pm0.01}$. This relationship indicates that the system has a liquidlike structural arrangement. The electrostatic interactions can be screened by addition of salt (NaCl). The short-range interactions between the dendrimer molecules were investigated by systematically varying the salt concentration in the solution. We demonstrate that the peak intensity decreases monotonically by increasing the salt concentration. In addition, this system shows a steep upturn in the scattered intensities at low wavevector reflecting the presence of large-scale structures, likely indicating aggregation of dendrimers or other inhomogeneous molecular distribution.

1. Introduction

Dendrimers are new kind of hyperbranched molecule with complex and controlled architecture.[1−3] The unusual properties of the molecules have sparked many potential applications ranging from organic synthesis to medical sciences.[4−6] The molecules are built by repetitive reaction steps starting from a central multifunctional core under systematic introduction of branching sites. Poly(propyleneimine) dendrimers, which are abbreviated as DAB-*dendr*-$(NH_2)_n$, are characterized by the parameter "n", the number of primary (terminal) amine groups in the outermost shell. The first generation ($n = 4$) is synthesized starting from 1,4-diaminobutane, to which four propyleneimine monomers are added.[7,8] Stepwise addition of propyleneimine monomers leads to dendrimers up to the fifth generation ($n = 8$, 16, 32, 64). The physical−chemical properties of such dendrimers can differ substantially from the behavior of linear polymers. It was found that the specific viscosity of the dendrimer solutions presents a maximum by varying the molecular weight, while this quantity is monotonically increasing for linear polymers. Such a property is typically related to the dendrimer branched structure, leading to compact molecules as compared to linear polymers.[2,9,10]

In polyelectrolyte dendrimers, Young and co-workers[11] and Briber and co-workers[12] found that the charge−charge repulsions can be minimized by separating the charged moieties as far apart as possible, leading to an expansion of the dendrimer arms and consequently a rearrangement of the dendrimer's density profile. Both studies show a change in the conformational properties of the dendrimers in solution by varying their pH. Using Monte Carlo simulations, Welch and Muthukumar[13] have studied the polyelectrolyte aspect of the dendrimers. They demonstrated that the shape of the intramolecular density profile of dendritic polyelectrolytes could be tailored by varying different parameters such as salt concentration or solvent pH.

In this article we focus on results from charged fifth generation poly(propyleneimine) dendrimers in solution. We have systematically varied the degree of ionization of the dendrimers by adding salt (NaCl) in order to follow the screening of the Coulombic interactions over a wide range of ionic strengths. In the Discussion section, we applied a theoretical model developed by Borue and Erukhimovich[14] based on weakly charged polyelectrolytes in a poor solvent to describe qualitatively our scattering data.

2. Experimental Section

2.1. Materials. Astramol dendrimers are made using diaminobutane as a core. They were synthesized by repetitive reaction sequence of Michael additions of acrylonitrile to the primary amine groups followed by hydrogenation of nitrile groups. More details concerning the synthesis are published elsewhere.[7,8] In the present work, we focus our investigation on the fifth generation dendrimers, DAB-*dendr*-$(NH_2)_{64}$, with 64 amine end groups. These dendrimers have been purified because they contain a very low amount (<1%) of nitrile end groups dendrimers, DAB-*dendr*-$(CN)_{64}$. This impurity can be removed in the following way: In a separation funnel 20 g of DAB-*dendr*-$(NH_2)_{64}$ dissolved in 10 mL of water is washed twice with 25 mL of chloroform. Phase separation into two layers after shaking takes about 6 h. The purified DAB-*dendr*-$(NH_2)_{64}$ is then obtained by removing water with a rotary evaporation for several hours. We notice that poly(propyleneimine) dendrimers are very pure compounds, as is evident from published analytical data, and they were used as received without any additional purification.[15,16]

2.2. Small-Angle Neutron Scattering (SANS). The small-angle neutron scattering measurements were carried out using

---

[†] Eindhoven University of Technology.

[‡] DSM Research.

[§] Risø National Laboratory.

* To whom correspondence should be addressed.

10.1021/ma011057o CCC: $22.00

the SANS facility at the Risø National Laboratory in Denmark. The covered scattering vectors, defined as $|\mathbf{Q}| = Q = (4\pi/\lambda)\sin(\theta/2)$, vary between 0.025 and 0.225 Å^{-1} with neutron wavelength resolution $\Delta\lambda/\lambda = 18\%$. ($\lambda$ is the neutron wavelength, θ is the scattering angle, and $\Delta\lambda$ is the full width at half-maximum value of the neutron flux vs wavelength distribution.) The neutrons are monochromatized by a mechanical selector. For each sample, the scattering patterns were obtained using the spectrometer configuration: $\lambda = 3$ Å, $D = 3$ m, and $L = 3$ m (L is the collimation length and D is the sample−detector distance).

The dendrimers were dissolved in deuterated water (D_2O, Campro Scientific) in a concentration range from 0.5% to 2% (v/v). The samples were measured at room temperature in rectangular quartz cells (Hellma) with path length of 2 mm. The data were radially averaged to reduce the statistical error. The scattering due to the empty cell and the solvent, as well as a calculated incoherent background caused by the protons, was subtracted. Thereafter, the neutron scattering intensity of the raw data is normalized with the scattering of 1 mm of water, H_2O, used as a standard. The water scattering was also used to determine the detector efficiencies. Finally, one obtains the coherent scattering cross section, $d\Sigma/d\Omega(Q)$, in absolute units (cm^{-1}). For simplicity, $d\Sigma/d\Omega(Q)$ will be denoted as $I(Q)$.

3. Results and Discussion

The scattering intensity $I(Q)$ from a homogeneous solution of monodisperse particles can be expressed as follows:[17,18]

$$I(Q) = KP(Q)\,S(Q) \tag{1}$$

where K (cm^{-1}) is the contrast factor, $P(Q)$ is the single particle form factor describing the intraparticle interference ($P(Q\rightarrow 0) = 1$), and $S(Q)$ is the interparticle interference (known as the solution structure factor).

The contrast factor is proportional to the particle volume fraction and depends on the difference of scattering length densities between the particles and the solvent.

$$K = \phi\,\frac{V_W}{N_A}\left(\frac{\sum_p b_i}{v_p} - \frac{\sum_s b_i}{v_s}\right)^2 \tag{2}$$

where N_A is the Avogadro constant and ϕ the volume fraction of the particles in solution (v/v). V_W (cm^3/mol) is the weight-average molar volume of the particles. Here $\sum_p$ and $\sum_s$ denote summation of the scattering lengths b_i (cm) of the different atoms in the particles, and v_p and v_s are the volumes of the particles and the solvent molecules, respectively.

For monodisperse spheres of radius R, the particle form factor is

$$P(Q) = \left[\frac{3[\sin(QR) - QR\cos(QR)]}{(QR)^3}\right]^2 \tag{3}$$

The radius of gyration R_g of the particles is given by $R_g = {}^3\!/_5 R$.

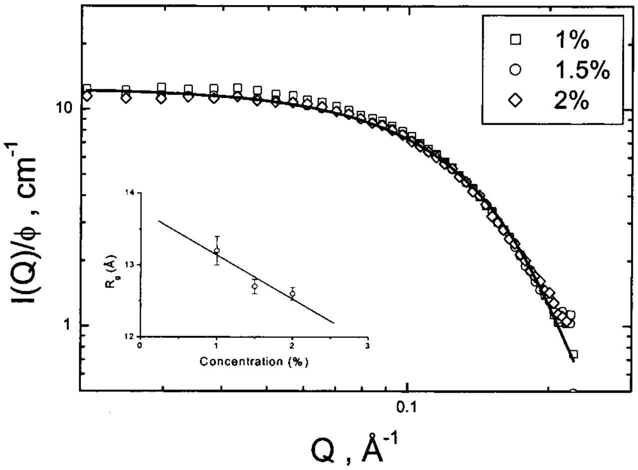

Figure 1. Scattered intensities, in log−log representation, from dilute solutions in D_2O prior adding acid as a function of dendrimers concentration. The scattering data are normalized by the dendrimer volume fractions. The inset curve shows R_g plotted vs the concentration obtained from the spherical model. The figure shows also the fit result of the scattered intensity from 1.5% dendrimers solution using monodisperse spheres form factor.

Table 1. Radius of Gyration of the Dendrimers Extracted from the Fit of the Scattered Intensities Using Guinier and Monodisperse Spheres Form Factors

concentration (%)	R_g (Å) sphere	R_g (Å) Guinier
1	13.2 ± 0.2	13.3 ± 0.2
1.5	12.7 ± 0.1	12.9 ± 0.1
2	12.6 ± 0.1	12.8 ± 0.1

Experimentally, for "dilute" polymer solutions (with no Coulombic interactions), intermolecular correlations can be ignored, leading the scattering information from individual molecules (size and shape). By extrapolating to zero concentration, $P(Q)$ can be obtained because the structure factor $S(Q) \rightarrow 1$. For nondilute solutions, the interference term $S(Q)$ can be obtained by dividing the total scattered intensity by $P(Q)$. In theory, the form factor corresponding to a given geometry and defined density distribution can be calculated. The calculation of interparticle interference term $S(Q)$ is not very obvious. For strongly interacting polymers in solution, for example for polyelectrolytes, the effect is much more dramatic. In the case of charged particles, the calculation requires complex models describing the effects of the long-range Coulombic interactions.

Figure 1 shows a double-logarithmic representation of the scattered intensity of dendrimer solutions in D_2O prior to adding the acid given as a function of dendrimer volume fraction in dilute regime; i.e., the interactions between the dendrimers are negligible ($S(Q) \sim 1$). The intensities were normalized to the solution concentrations in order to allow a direct comparison. The data were analyzed using either eq 3 or the classical Guinier approximation $P(Q) = \exp(-Q^2R_g^2/3)$, yielding the apparent radius of gyration R_g of the dendrimers. The scattering curve obtained from the solution of 1.5% concentration is fitted quite well over the range of scattering angles by the model calculation for monodisperse spheres without interaction (Figure 1) as well as the Guinier function. The values of R_g, listed in Table 1, are in good agreement with the previous SANS experiments.[9,19] We notice that the slight decrease of R_g for the three concentrations is due to virial effects. The inset curve shows R_g plotted vs the concentration.

By adding acid HCl to a dendrimer solution, a distinct correlation peak appears in the scattering intensity indicating long-range Coulombic interactions due to the charges in the dendrimers (Figure 2). The characteristic scattering vector Q^* changes markedly with concentration. The amount of 10 M HCl present in the solution is related to the parameter α, called the *protonation degree*, defined as the ratio between the number of protons added and the total number of *tertiary* and *primary* amine groups (62 tertiary and 64 primary) in

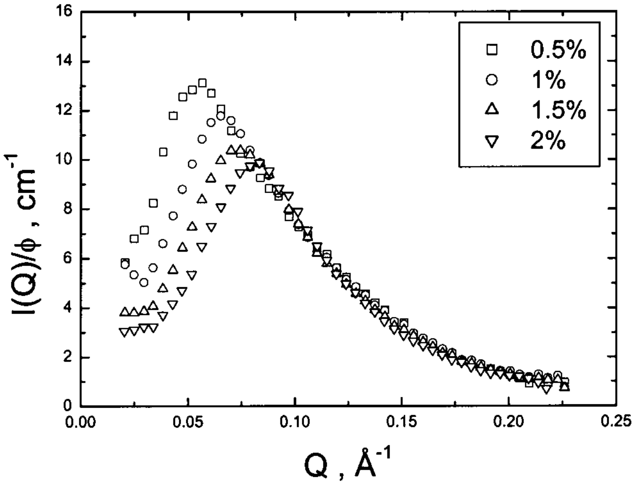

Figure 2. Effect of dendrimer concentration on the scattering patterns from solutions of charged dendrimers with $\alpha = 0.25$. The symbols correspond to $\phi = 0.5\%$ (squares), 1% (circles), 1.5% (triangles up), and 2% (triangles down). The data are normalized by the dendrimer volume fractions.

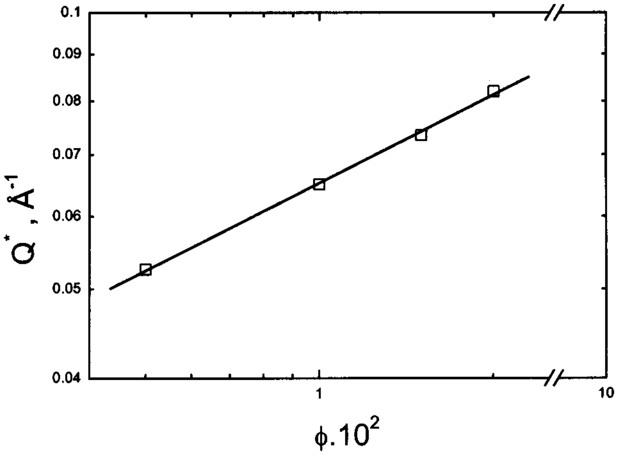

Figure 3. Variation of the peak position Q^* against the dendrimers concentration with $\alpha = 0.25$. The solid line represents the fit of the data with a power law.

the dendrimer. The osmotic pressure of the solution is higher than the initial solution in pure D_2O and the decrease of the scattering intensity at low *Q* values, ignoring the upturn at very low *Q*, which will be discussed later in this paper, is essentially due to the increase of the osmotic compressibility induced by the protonation of dendrimer molecules. Figure 2 shows the effect of dendrimer concentration on the scattering patterns for fixed protonation degree $\alpha = 0.25$. One observes that the peak position is shifting to higher *Q* values as the dendrimer concentration increases. For more qualitative analysis, the values of Q^* are plotted as a function of dendrimer volume fraction as illustrated in Figure 3. A nonlinear least-squares fit to the data shows that Q^* scales as ϕ^β with $\beta = 0.32 \pm 0.01$. Quantitatively, the value of the scaling exponent is in good agreement with the model proposed by Guinier and Fournet,[20] based on the arrangement of particles in distorted face-centered-cubic lattice ($\beta = {}^1/_3$), and the experimental results on PAMAM dendrimers.[21]

As mentioned by Guinier and Fournet, the peak position depends on the structure of the particle's arrangement and on the particular structure of each particle.[20] Its position can be related to the so-called "Bragg distance" defined as $d^* \equiv 2\pi/Q^*$. In the present study, we notice that the average distance between the particle centers d^* increases from 77 to 120 Å upon decreasing the dendrimer volume fraction from 2% to 0.5%. One remarks that the interparticle distance values are almost an order of magnitude larger than the size of the uncharged particles. We emphasize that the Bragg peak in the acidified system does not originate from the excluded volume between the dendrimers as observed in our previous study[19] for high-concentration solutions in pure D_2O (i.e., before adding HCl).

Table 2. Values of the Peak Position and Their Corresponding Bragg Distance between the Dendrimers in Solution at Different Concentrations with $\alpha = 0.25$[a]

concn (%)	Q^* (Å^{-1})	$d^* = 2\pi/Q^*$ (Å)	α_s	$I(Q^*)$ (cm^{-1})
0.5	0.056	112.2	0	0.066
0.05	0.060			
0.25	0.058			
1	0.065	96.7	0	0.118
0.05	0.106			
0.25	0.103			
1.5	0.074	85.0	0	0.155
0.05	0.142			
0.25	0.140			
2	0.083	75.7	0	0.217
0.05	0.180			
0.25	0.175			

[a] The values of the peak intensities are included as a function of the neutralization degree α_s.

In the previous paper,[19] we have demonstrated that the screening of the Coulombic interactions in acidified solutions can be accomplished by addition of salt (NaCl). The dimensionless parameter α_S, defined as the salt concentration, is called the *neutralization degree*.[22] The scattering patterns of a set of dendrimer solutions with four different concentrations ϕ (0.5%, 1%, 1.5%, and 2%) have been measured (Figure 4). The protonation degree is maintained constant $\alpha = 0.25$, but the added salt concentrations vary between 0 and 0.5. In Figure 4, the scattered intensities $I(Q)$ are plotted as a function of *Q*.

We first note that all patterns superimpose at high *Q* ($Q \geq 0.1$ Å^{-1}) where the intensity reflects essentially the form factor $P(Q)$ of dendrimers ($S(Q) \rightarrow 1$). This provides the information about the local structure within the dendrimer molecule and implies that the internal structure is not influenced significantly by the intermolecular interactions (neither the excluded volume nor the Coulombic interactions). This internal structure remain unchanged up to the spatial resolution of our scattering experiments $r \sim \pi/0.1$ Å^{-1} = 30 Å. Furthermore, for all solution concentrations (Figure 4), a very distinct and broad peak is observed in the scattering intensity in the "salt free" case ($\alpha_S = 0$). The addition of a small amount of salt (NaCl) to the charged dendrimer solution decreases the peak intensity while its position is roughly maintained unchanged. However, a progressive screening of electrostatic forces is observed when α_s increases, but the Bragg distance d^* does not change with ionic strength. Table 2 summarizes the Bragg peak values Q^* and their corresponding Bragg distances d^* at different dendrimer concentrations ϕ. The values of the peak intensity $I(Q^*)$ are also included as a function of the neutralization degree α_s. Those values cannot be extracted accurately from the scattered intensities for larger amount of added salt ($\alpha_s > 0.25$) because of the broadness of the peak. When enough salt is added, the scattering intensity at zero angle $I(Q \rightarrow 0)$ remains smaller than that of dendrimer solutions in pure D_2O, and no peak is observed in the scattering

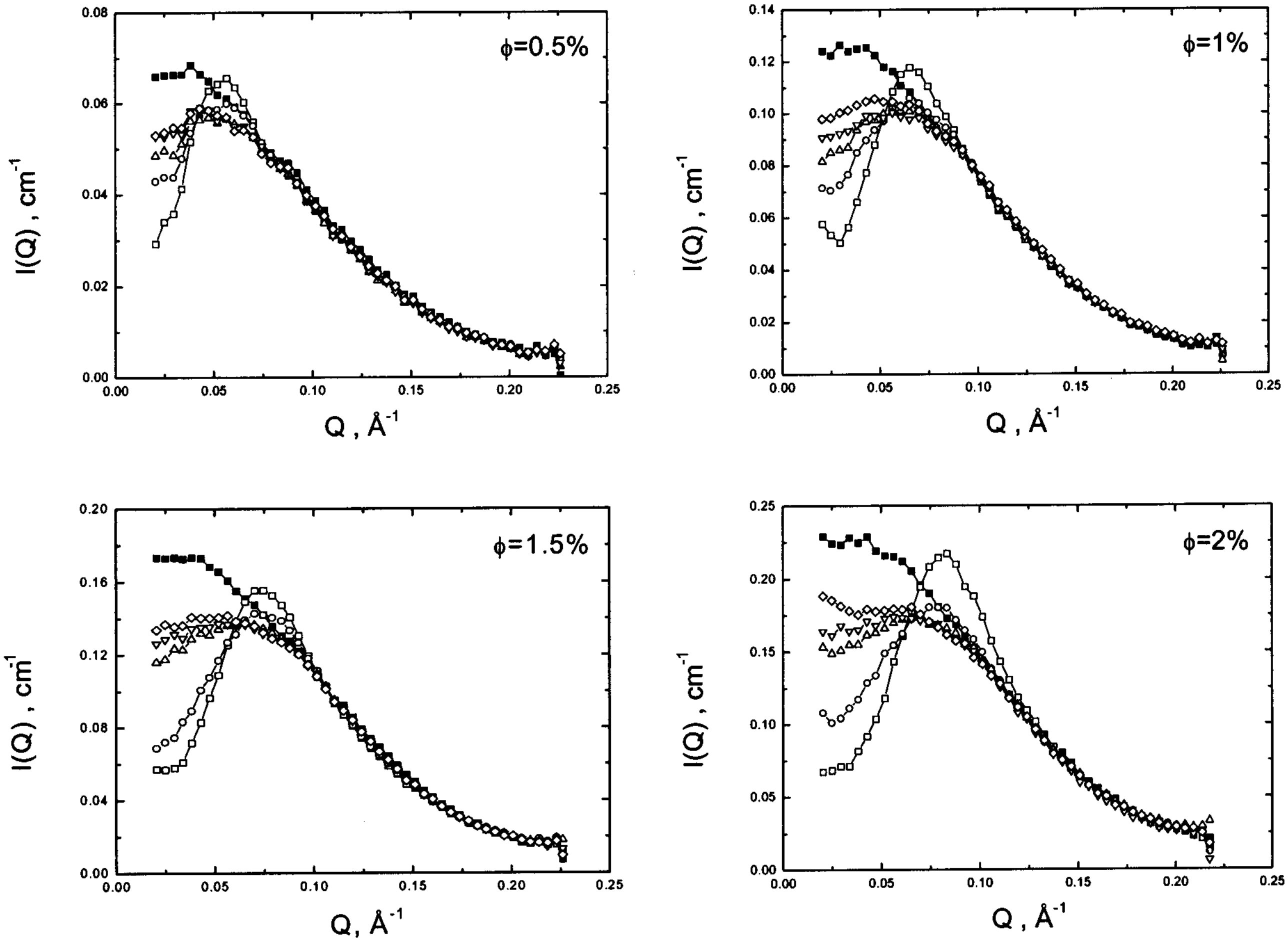

Figure 4. Effect of the addition of salt NaCl to the scattering patterns from charged ($\alpha = 0.25$) dendrimer solutions at different concentrations ϕ (0.5%, 1%, 1.5%, and 2%). The symbols correspond to $\alpha_S = 0$ (squares), 0.05 (circles), 0.25 (triangles up), 0.35 (triangles down), and 0.5 (diamonds). The filled squares represent the scattering intensity of the dendrimers in pure D_2O ($\alpha = 0$, $\alpha_s = 0$).

patterns. Such an effect might be due to the increase of the osmotic compressibility by adding a large excess of salt, caused probably by the increase of the total concentration of the solution. One notices that the data of the acidified solutions with large amount of salt cannot be well fitted by the previous models, i.e., Guinier function and monodisperse spherical form factor. Thus, the radius of gyration cannot be determined correctly from these data.

The constancy of the peak position upon adding salt has been reported by several authors[23–29] with, however, differing interpretation, as we discuss below. For $Q < Q^*$, the scattering intensity is very sensitive to the addition of salt, and for $Q > Q^*$, $I(Q)$ preserves a level of scattering close to the value in the absence of salt as expected by most theoretical models for electrostatic interactions in the semidilute range of concentration. It is finally interesting to note that there is a sort of "isosbestic" point located at roughly $Q = Q_{\mathrm{cross}} = 0.065$ $\mathrm{Å}^{-1}$ for solution concentration of 2% ($Q_{\mathrm{cross}} = 0.042$, 0.056, and 0.061 $\mathrm{Å}^{-1}$ for concentrations of 0.5%, 1%, and 1.5%, respectively) where all the intensities are independent of the salt concentration. Similar results have been obtained in various polyelectrolyte system.[30] So far, no theoretical model has been formulated to explain this observation, although it is common to several different polyelectrolyte systems.[27,31]

Our results concerning the effect of salt on the peak position discussed above differ from those reported by many authors.[32–35] For example, the SAXS results of Wang and Bloomfield[35] on DNA system show a peak position that is strongly dependent on the added salt concentration. Their interpretation given for this dependence is related to the occurrence of a kind of transition, from hexagonal packing to a uniform distribution, of the molecules upon adding salt. One notices that the effect of salt on the peak position is still not very well understood. Different systems, and sometimes even similar systems, show different behaviors when changing the solvent quality, for example, leading to different interpretations and speculations. Some studies on PAMAM dendrimers have shown the same results as those in the present work.[21]

One can evaluate the effect of added salt to a charged dendrimer solution via the structure factor $S_{\mathrm{salt}}(Q)$ by dividing the total intensity $I(Q)$ by the dendrimer's salt free form factor $P(Q)$, assuming that the form factor to first approximation is unaffected by the addition of salt. Figure 5 illustrates such effect for the lowest and the highest dendrimer concentrations $\phi = 0.5\%$ and 2%. As a first approximation, we used the scattered intensity from the solution in pure D_2O, i.e., $\alpha = 0$ and $\alpha_s = 0$, as the dendrimer's form factor.[36] With no salt added, the pair correlation function of a protonation degree $\alpha = 0.25$ dendrimer solution shows a well-developed first-order maximum. However, introduction of salt dramatically alters the scattering profile.

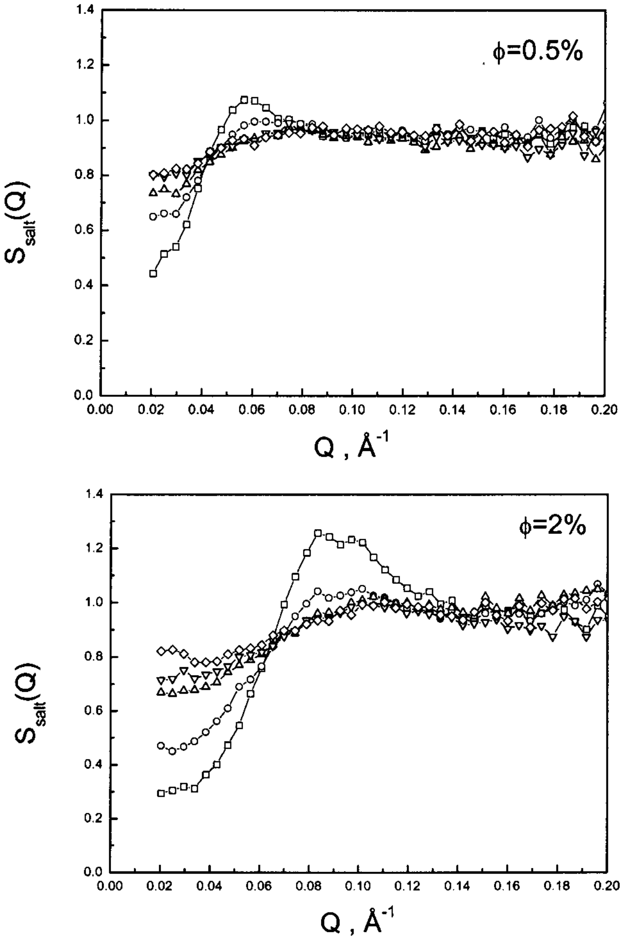

Figure 5. Concentration dependence of the structure factor $S_{salt}(Q)$ extracted from the SANS scattered intensities from 0.5% and 2% charged ($\alpha = 0.25$) dendrimers solutions. The symbols correspond to $\alpha_s = 0$ (squares), 0.05 (circles), 0.25 (triangles up), 0.35 (triangles down), and 0.5 (diamonds).

According to polyelectrolyte theory,[37-39] salt adds to inverse Debye lengths via $K_t^2 = K_p^2 + K_s^2$, where the total screening length K_t^{-1} is composed of the screening parameter K_s^{-1} for the added salt and K_p^{-1} for the counterions released from the polyions. As a result, the screening structure factor peak diminishes in height and broadens as effective interactions are screened. A substantial jump in the low Q intensity also occurs as α_s increases. This is a classic feature of polyelectrolyte solutions and is caused by the increase in the osmotic compressibility within the systems as mentioned in the previous paragraph. Since the low Q scattering is described by $S(Q) = k_BT(\mathrm{d}\Pi/\mathrm{d}\phi)_T^{-1}$, it becomes clear why the scattering intensity at $Q \to 0$ becomes severely less depressed, and the system tends to return to the typical dilute solution behavior without charges. These trends appear to be universal features of polyelectrolyte solutions, having been observed for linear as well as spherical polyions.[39]

It is important to notice that a starting of an upturn in the scattering data has been observed at low Q as shown in Figure 6. Typically, the low Q upturn and an intensity maximum are two features commonly observed in SAXS and SANS measurements on linear polyelectrolytes.[25,28,40-48] Reports of this upturn, reflecting some kind of large-scale inhomogeneity, are, on the other hand, rather rare for spherical polyions.[49,50] While the Q^* can be attributed to macroion ordering, the low

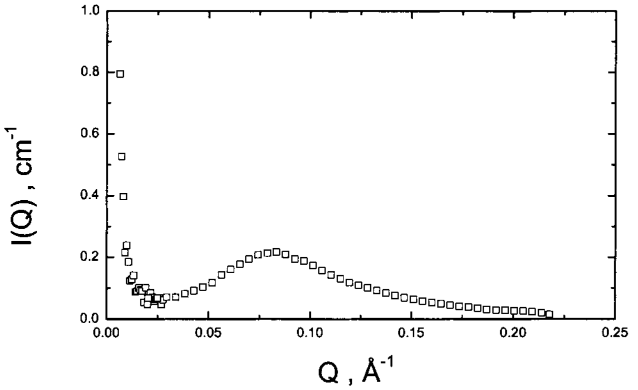

Figure 6. SANS scattered intensity plotted vs Q for 2% charged dendrimer solution with $\alpha = 0.25$ before adding salt ($\alpha_s = 0$). The figure illustrates the upturn in the scattering intensity at low Q.

Q upturn is not well understood, and there is still a lack of understanding of its physical meaning. Part of difficulty in interpreting this feature is due to the fact that it occurs at Q values typically at the lower limit of SAXS and SANS measurements. It is important to notice the presence of the upturn at low Q in the scattered intensities of the charged systems represented in Figures 2, 4, and 5. The upturn was not included in those figures because the SANS measurements were carried out only on a few solutions.

Some previous investigations[51] have taken the upturn at low Q as evidence of incipient macroscopic demixing promoted by hydrophobic interactions in aqueous solutions. Recent static light scattering[28,52] studies on aqueous polyelectrolyte solutions have shown that large-scale structures are present. These structures were demonstrated to be much larger than the size of single chains and were therefore attributed to multichain domains. Similar studies have been carried out on polyelectrolyte solutions of DNA using SANS. It was reported that this behavior at low Q could be related to the presence of local inhomogeneities in the solution.[30] The nature of the low Q data and the physical interpretation of the upturn still constitute a challenging problem.

Another model has been developed by Förster et al.[28] in which they explain the low Q upturn observed in aqueous semidilute solutions of quaternized poly(2-vinylpyridine) with low salt fraction. It was proposed in this model that temporal and disordered domains of high polymer concentration freely diffuse within an ordered and transient polyelectrolyte network. This model was inspired from the isotropic model of de Gennes et al.[53] in which they have introduced a second length scale, which, however, according to the experiments are of wrong size.

Roij, Dijkstra, and Hansen[54] proposed a so-called "volume term" model to explain the phase separation in charge-stabilized colloidal suspensions. The system is assumed to be composed of highly charged spherical polyions and microscopic co-ions and counterions dissolved in water. They demonstrate that a fluid–fluid (or gas–liquid) phase separation for sufficiently low ionic strength may occur in charge-stabilized colloidal particles in which the particle–particle interaction is purely repulsive rather than attractive. It was pointed out also that the increase of the scattered intensity at low Q is due to a fluid–fluid phase separation caused by an enhancement of the density fluctuations near the critical point. Langmuir[55] was the first who suggested the possibility of a fluid–fluid phase separation of suspensions or solutions of charged polyions.[55] His approach purely qualitative was based on the behavior of the osmotic pressure, evaluated within Debye–Hückel theory for simple electrolytes.[56]

In the "two-state structures" model, Ise has interpreted the low Q upturn by the presence of ordered domains of a higher polymer density within a less dense disordered solution.[42,45] Similar behavior has been observed experimentally on charged latex dispersions, and microscope images of charged lattices show the existence of an order–disorder tow-state solution structure,[57] confirmed by ultrasmall-angle X-ray scattering (USAXS) measurements.[46,50]

More recently, Schmitz and Bhuiyan[58] have demonstrated that a phase separation in "two-state" colloidal systems occurs because of the contribution of both attractive and repulsive interactions as in the Sogami–Ise theory.[59] The attractive term was attributed to the electrostatic osmotic pressure. Such model provides other explanation of the origin of the heterogeneities observed experimentally in colloidal suspensions.

Borue and Erukhimovich have developed a model based on weakly charged linear polyelectrolytes in a poor solvent.[14] This model, which considers the polyelectrolyte solution as a three-component system composed of macroions, counterions, and solvent, is based on the random phase approximation (RPA) formalism of a semidilute solution. The polyelectrolyte chains follow the "electrostatic blobs" approach as described by many authors.[53,60,61] Consequently, the local conformation within the blobs is weakly influenced by the electrostatic interactions but dominated by the subunit–solvent interactions. Because of lack of more appropriate models available for the polyelectrolyte dendrimers, we will attempt to analyze our data with this model, being aware that some fitting parameters might become quite unrealistically. Using the RPA approach, the calculated scattering function, which has been used by many authors[62] in the analysis of the SANS data, is given by

$$S(Q) = \frac{C}{4\pi l_B {r_0}^2 \alpha^2} \frac{x^2 + s}{(x^2 + s)(x^2 + t) + 1} \tag{4}$$

where C is a scaling constant, x is the reduced scattering vector, t is the reduced temperature, s is the reduced charge concentration, and r_0 represents the characteristic scale of the electrostatic screening related to the parameter x by

$$x = r_0 Q \tag{5}$$

with

$$r_0 = a\left(\frac{48\pi l_B}{a}\phi\alpha^2\right)^{-1/4} \tag{6}$$

with a being the segment length, l_B the Bjerrum length, α the charge density, and ϕ the polymer volume fraction. The reduced charge concentration s is related to the Debye screening length κ^{-1} as

$$s = \kappa^2 {r_0}^2 \tag{7}$$

The reduced temperature t depends on the solvent quality: $t > 0$ for good solvent and $t < 0$ for poor solvent.

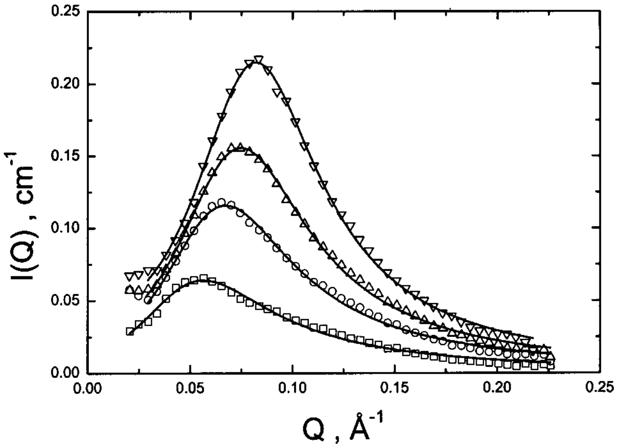

Figure 7. Fit results of the scattered patterns of Figure 2 using Borue and Erukhimovich model. The symbols correspond to $\phi = 0.5\%$ (squares), 1% (circles), 1.5 (triangles up), and 2% (triangles down). The low Q values are excluded in the fit.

Table 3. Parameters Extracted from Borue and Erukhimovich Function Fit of the Scattered Intensities from an Acidified Solutions at a Protonation Degree $\alpha = 0.25$

concn (%)	C (barns)	a (Å)	κ^{-1} (Å)	h (Å^3)
0.5	137 ± 23	1.40 ± 0.10	40 ± 6	586 ± 144
1	113 ± 12	1.37 ± 0.06	32 ± 3	895 ± 24
1.5	80 ± 7	1.30 ± 0.04	25 ± 1	868 ± 18
2	55 ± 4	1.13 ± 0.03	19 ± 1	763 ± 19

It is given by

$$t = -12\left(\frac{r_0}{a}\right)^2\left(\frac{h}{a^3}\right)\phi \tag{8}$$

where h is the third virial coefficient.

Using eq 4, we show in Figure 7 the fit results of the scattered intensities from acidified dendrimer solutions with $\alpha = 0.25$ at four concentrations: $\phi = 0.5\%$, 1%, 1.5%, and 2%. The variables C, a, κ, and h were taken as adjustable parameters. One notices that Borue and Erukhimovich model fits quite well our data if the low angle values are ignored while the fits become poor if we include Q values below $Q \sim 0.03$ Å^{-1}. In this case, the calculated curves describe the experimental data in shape, position, and height of the peak, indicating the dominance of the long-range electrostatic interactions in charged dendrimer molecules. The results of the fit are listed Table 3. It is important to notice that the values of these fitted parameters, as mentioned above, might be unrealistic since the model of Borue and Erukhimovich is originally appointed to study weakly charged polyelectrolytes, i.e., linear chains. We will anyway discuss the parameters in some detail: The screened Debye length shows reasonable concentration dependence, decreasing from 40 Å at 0.5% to 19 Å at 2.0%. The third virial coefficient shows a monotonic decrease in the 1–2% range, which seems reasonable, however, with a peak value near 1%. This is unexpected and could reflect the limitation of the model.

4. Conclusion

In this work, small-angle neutron scattering has been performed on solutions of generation G5 of poly(propyleneimine) dendrimers in D_2O. The dendrimers were acidified by adding acid (HCl), and the scattering intensities exhibit a single correlation peak indicating a spatial arrangement of the molecules in the acidified medium due to the electrostatic repulsion. Its position scales with the dendrimers volume fraction with an exponent of 0.32 ± 0.01, indicating that the system has a liquidlike ordering. These electrostatic interactions can be screened by addition of salt (NaCl). The peak intensity in the scattered intensities decreases monotonically by increasing the salt concentration. Furthermore, the scattered intensity from acidified dendrimer solutions containing an excess of salt does not reach the scattering from the neutral solution (initial solution in pure D_2O). This could be due to the increase of the osmotic compressibility of the neutralized solution, after adding an excess of salt, caused by an increase of its total concentration (i.e., dendrimers and salt concentration in the solution).

In addition to the peak discussed above, there is a distinct upturn of scattered intensity in the very small Q range (typically, $Q < 0.03$ Å^{-1}). Similar behavior has been observed in the SANS data in other systems, for instance, flexible polyelectrolytes (PSSNa)[25] and polysaccharides.[27] This upturn indicates the presence of structures larger than single molecules leading to multidendrimer domains.

A model used to explain the physics of such systems must explain all these features (i.e., presence of the correlation peak and the upturn at low Q). Unfortunately, no current model meets this challenge, and only if the data at lowest angles are ignored can the calculated intensity derived from the model of weakly charged polyelectrolytes in a poor solvent fit our scattering data.

References and Notes

(1) Tomalia, D. A.; Baker, H.; Dewald, J.; Hall, M.; Kallos, G.; Martin, S.; Roeck, J.; Smith, P. *Polym. J.* **1985**, *17*, 117.
(2) Tomalia, D. A.; Naylor, A. M.; Goddard, W. A., III *Angew. Chem., Int. Ed. Engl.* **1990**, *29*, 138.
(3) Newkome, G. R.; Moorefield, C. N.; Baker, G. R.; Johnson, A. L.; Behera, R. K. *Angew. Chem., Int. Ed. Engl.* **1991**, *30*, 1176.
(4) Bielinska, A.; Kukowska-Latallo, J. F.; Johnson, J.; Tomalia, D. A.; Baker, J. R. Jr. *Nucleic Acids Res.* **1996**, *24*, 2176.
(5) Tomalia, D. A.; Durst, H. D. *Top. Curr. Chem.* **1993**, *165*, 193.
(6) Fréchet, J. M. J. *Science* **1994**, *263*, 1710.
(7) de Brabander, E. M. M.; Meijer, E. W. *Angew. Chem.* **1993**, *105*, 1370.
(8) de Brabander, E. M. M.; Brackman, J.; Mure-Mak, M.; de Man, H.; Hogeweg, M.; Keulen, J.; Scherrenberg, R.; Coussens, B.; Mengerink, Y.; van der Wal, S. *Macromol. Symp.* **1996**, *102*, 9.
(9) Scherrenberg, R.; Coussens, B.; van Vliet, P.; Edouard, G.; Brackman, J.; de Brabander, E. M. M.; Mortensen, K. *Macromolecules* **1998**, *31*, 456.
(10) Morikawa, A.; Kamimoto, M.; Imai, Y. *Macromolecules* **1991**, *24*, 3469.
(11) Young, J. K.; Baker, G. R.; Newkome, G. R.; Morris, K. F.; Johnson, C. S. *Macromolecules* **1994**, *27*, 3464.
(12) Briber, R.; Bauer, B.; Hammouda, B.; Tomalia, D. *Polym. Mater. Sci. Eng.* **1992**, *67*, 430.
(13) Welch, P.; Muthukumar, M. *Macromolecules* **1998**, *31*, 5892.
(14) Borue, V. Yu.; Erukhimovich, I. Ya. *Macromolecules* **1988**, *21*, 3240.
(15) Hummelen, J. C. *Chem. Eur. J.* **1997**, *3*, 1487.
(16) van der Wal, S. *J. Chromatogr.* **1998**, *A 825*, 135.
(17) Higgins, J. S.; Benoit, H. *Polymer and Neutrons Scattering*; Clarendon Press: Oxford, England, 1994.
(18) The scattering intensity takes this form if the particles have spherical shape or, at least on average, the interaction potential between them has spherical symmetry.
(19) Ramzi, A.; Scherrenberg, R.; Brackman, J.; Joosten, J.; Mortensen, K. *Macromolecules* **1998**, *31*, 1621.
(20) Guinier, A.; Fournet, G. In *Small Angle Scattering of X-Rays*; John Wiley and Sons: London, 1955.
(21) Nisato, G.; Ivkov, R.; Amis, E. J. *Macromolecules* **1999**, *32*, 5895.
(22) The neutralization degree α_s is defined as the stoichiometric ratio of added salt NaCl to the number of protons added through HCl in solution.
(23) Hayter, J.; Jannink, G.; Brochard, F.; de Gennes, P. G. *J. Phys., Lett.* **1980**, *41*, L-451.
(24) Ise, N. *Angew. Chem., Int. Ed. Engl.* **1986**, *25*, 323.
(25) Nierlich, M.; Williams, C. E.; Boué, F.; Cotton, J. P.; Daoud, M.; Farnoux, B.; Jannink, G.; Picot, C.; Moan, M.; Wolff, C.; Rinaudo, M.; de Gennes, P. G. *J. Phys. (Paris)* **1979**, *40*, 701.
(26) Drifford, M.; Dalbiez, J. P. *J. Phys. Chem.* **1984**, *88*, 5368.
(27) Morfin, I.; Reed, W.; Rinaudo, M.; Borsali, R. *J. Phys. II* **1994**, *4*, 1001.
(28) Förster, S.; Schmidt, M.; Antonietti, M. *Polymer* **1990**, *31*, 781.
(29) Maier, E. E.; Krause, R.; Deggelmann, M.; Hagenbtchle, M.; Weber, R.; Fraden, S. *Macromolecules* **1992**, *25*, 1125.
(30) Borsali, R.; Nguyen, H.; Pecora, R. *Macromolecules* **1998**, *31*, 1548.
(31) Xiao, L.; Reed, W. F. *J. Chem. Phys.* **1991**, *94*, 4568.
(32) Ise, N.; Okubo, T.; Kunugi, S.; Matsuoka, H.; Yamamoto, K.; Ishii, Y. *J. Chem. Phys.* **1984**, *81*, 3294.
(33) Ise, N.; Okubo, T.; Kunugi, S.; Yamamoto, K.; Matsuoka, H.; Kawai, H.; Hashimoto, T.; Fujimura, M. *J. Chem. Phys.* **1983**, *78*, 541.
(34) Ise, N.; Okubo, T.; Yamamoto, K.; Kawai, H.; Hashimoto, T.; Fujimura, M.; Hiragi, Y. *J. Am. Chem. Soc.* **1980**, *102*, 7901.
(35) Wang, L.; Bloomfield, V. *Macromolecules* **1991**, *24*, 5791.
(36) We used the scattered intensity corresponding to $\phi = 2\%$ as the dendrimer's form factor.
(37) Schmitz, K. S. *Langmuir* **2000**, *16*, 2115.
(38) Sanghiran, V.; Schmitz, K. S. *Langmuir* **2000**, *16*, 7566.
(39) *Macroions in Solution and Colloidal Suspension*; Schmitz, K. S., Ed.; VCH Publishers: New York, 1993.
(40) Moan, M. *Appl. Crystallogr.* **1978**, *11*, 519.
(41) Matsuoka, H.; Ise, N.; Okubo, T.; Kunugi, S.; Tomiyama, H.; Yoshikawa, Y. *J. Chem. Phys.* **1985**, *83*, 378.
(42) Matsuoka, H.; Schwahn, D.; Ise, N. *Macromolecules* **1991**, *24*, 4227.
(43) van der Maarel, J. R. C.; Groot, L. C. A.; Hollander, J. G.; Jesse, W.; Kuil, M. E.; Leyte-Zuiderweg, L. H.; Mandel, M.; Cotton, J. P.; Jannink, G.; Lapp, A.; Farago, B. *Macromolecules* **1993**, *26*, 7295.
(44) Boué, F.; Cotton, J. P.; Lapp, A.; Jannink, G. *J. Chem. Phys.* **1994**, *101*, 2562.
(45) Matsuoka, H.; Schwahn, D.; Ise, N. In *Macroion Characterization: from Dilute Solutions to Complex Fluids*; Schmitz, K. S., Ed.; ACS Symposium Series 548; American Chemical Society: Washington, DC, 1994.
(46) Essafi, W.; Lafuma, F.; Williams, C. E. In *Macroion Characterization: from Dilute Solutions to Complex Fluids*; Schmitz, K. S., Ed.; ACS Symposium Series 548; American Chemical Society: Washington, DC, 1994.
(47) Borsali, R.; Rinaudo, M.; Noirez, L. *Macromolecules* **1995**, *28*, 1085.
(48) Milas, M.; Rinaudo, M.; Duplessix, R.; Borsali, R.; Lindner, P. *Macromolecules* **1995**, *28*, 3119.
(49) Matsuoka, H.; Kakigami, K.; Ise, N. *Proc. Jpn. Acad.* **1991**, *67B*, 170.
(50) Matsuoka, H.; Kakigami, K.; Ise, N. *Proc. Natl. Acad. Sci. U.S.A.* **1991**, *88*, 6618.
(51) Shibayama, M.; Tanaka, T. *J. Chem. Phys.* **1995**, *102*, 9392.
(52) Sedlak, M.; Amis, E. J. *J. Chem. Phys.* **1992**, *96*, 817.
(53) de Gennes, P. G.; Pincus, P.; Velasco, R. M.; Brochard, F. *J. Phys. (Paris)* **1976**, *37*, 1461.
(54) van Roij, R.; Dijkstra, M.; Hansen, J.-P. *Phys. Rev. E* **1999**, *59*, 2010.
(55) Langmuir, I. *J. Chem. Phys.* **1938**, *6*, 873.
(56) Debye, P.; Hückel, E. *Physik. Z.* **1924**, *25*, 97.
(57) Ito, K.; Nakamura, H.; Yoshida, H.; Ise, N. *J. Am. Chem. Soc.* **1988**, *110*, 6955.
(58) Schmitz, K. S.; Bhuiyan, L. B. *Phys. Rev. E* **2001**, *63*, 011503-1.
(59) Sogami, I.; Ise, N. *J. Chem. Phys.* **1984**, *81*, 6320.
(60) Pfeuty, P. J. *J. Phys., Colloq. C2* **1978**, *39*, 149.
(61) Khokhlov, A. R. *J. Phys. A: Math. Gen.* **1980**, *A13*, 979.
(62) Moussaid, A.; Schosseler, F.; Munch, J. P.; Candau, S. J. *J. Phys. II* **1993**, *3*, 573.

MA011057O